Technical Physics, Vol. 50, No. 6, 2005, pp. 719–726. Translated from Zhurnal Tekhnicheskoĭ Fiziki, Vol. 75, No. 6, 2005, pp. 46–53.

OPTICS, QUANTUM ELECTRONICS

Er^{3+} Ion Photoluminescence in Silicate Glasses Obtained by Plasma-Chemical Deposition in a Low-Pressure Microwave Discharge

A. V. Kholodkov and K. M. Golant

Research Center of Fiber Optics, Prokhorov General Physics Institute, Russian Academy of Sciences, Moscow, 119991 Russia

e-mail: artem@fo.gpi.ru

Received April 21, 2004

Abstract—The luminescent properties of Er^{3+} ions embedded in silicate glass matrices with F, N, K, Al, P, Ge, P + Al, P + K, and Ge + Al admixtures are studied. Glass samples with an erbium concentration of up to 9×10^{20} cm^{-3} are synthesized by plasma-assisted CVD. The spectra, kinetics, and relative quantum efficiency of Er^{3+} photoluminescence are estimated by exciting the samples with 514.5-nm Ar^+ laser radiation. It is shown that the luminescent properties of the activator in such high-erbium unfused glasses are superior to those of the same activator in fused glasses of the same composition. This effect is attributed to suppression of clustering in the glasses prepared by low-temperature CVD, which arises because of a limited mutual solubility of the oxides in the melt. The efficient composites with an erbium concentration of up to 4×10^{20} cm^{-3} obtained in this work can be used as an active medium of waveguide lasers and amplifiers. © *2005 Pleiades Publishing, Inc.*

INTRODUCTION

The Er^{3+} ion is widely used as an activator in fiber-optic amplifiers and lasers, since the luminescence band of the $^4I_{13/2}$–$^4I_{15/2}$ metastable laser transition falls into the basic telecommunication range near 1.55 μm. However, the intrinsically high efficiency of these lasers and amplifiers declines with an increase in the activator concentration because of the well-known clustering effect. As a result, the production of high-quantum-efficiency Er^{3+}-doped active optical waveguides that meet the requirements of integrated optics becomes a challenging task. The advantages of integrated optical circuits over fiber-optic ones are a low amount of manual labor (all circuit features are made by lithography), small size, and low cost.

To make active elements based on short-optic-path waveguides, it is necessary that the activator ion concentration in the glass be one order of magnitude higher than in the fibers. However, as the activator ion concentration grows, the mean ion spacing shrinks and additional channels of excitation relaxation become significant. One of these channels is associated with the up-conversion effect [1, 2]: interaction of two nearby excited erbium ions with subsequent nonradiative relaxation of one of them [3]. In fused glasses, including silica fibers, the reason for a sharp increase in the concentration of pairs of nearby Er^{3+} ions with increasing erbium concentration is the poor solubility of Er_2O_3 in SiO_2.

The up-conversion effect observed at elevated concentrations of the activator can be combated in two ways, either eliminating various reasons for the effect (for details, see [4]). The former way is to introduce Al, P, or alkali metals into the SiO_2 matrix. These admixtures loosen the structural network of the glass, thereby reducing the rate of excitation migration between Er^{3+} ions and improving the erbium solubility. The latter way is to apply low-temperature (without fusion) CVD synthesis of the glass, which makes activator ions statistically uniformly build in the glass network, thus preventing the formation of erbium clusters. Clearly, the combination of these approaches will provide the highest efficiency in suppressing up-conversion.

Today, magnetron sputtering, ion implantation, and plasma-chemical deposition are the most popular techniques for obtaining unfused glasses in the form of planar Er-doped layers [5, 6]. The glass formation temperature in these techniques varied from 300 to 500°C. However, the "refinement" of the film structure takes place, as a rule, upon additional annealing at ≈1000°C.

Of special interest among these techniques is surface plasma-chemical vapor deposition (SPCVD) [7], which forms a transparent glass layer at substrate temperatures in the range 1000–1200°C. In this case, increased process temperatures make subsequent annealing unnecessary. A significant advantage of SPCVD is a higher rate of glass deposition compared with the other techniques. It was shown [8] that the SPCVD may serve as a technological platform for creating active integrated optical waveguides.

1063-7842/05/5006-0719$26.00 © 2005 Pleiades Publishing, Inc.

In this work, we investigated the luminescence due to Er ions embedded in SPCVD-grown bulk unfused glasses of different composition to a concentration of 9×10^{20} cm^{-3}. The luminescence spectra and kinetics were studied at wavelengths of 0.98 and 1.53 μm. Identical conditions of luminescence excitation and recording made it possible to compare the quantum efficiency of excitation of the $^4I_{13/2}$–$^4I_{15/2}$ radiative transition in the glasses.

EXPERIMENTAL

The doped glasses used were deposited on the inner surface of quartz silica tubes using a setup intended for preparation of preforms for fiber drawing. In this version of the SPCVD process, a halogenide–oxygen mixture kept at a pressure of 0.5 Torr is applied through a tube of diameter 20 mm (a wall thickness of 2 mm) toward a stationary plasma column. The column is sustained inside the tube by surface microwave plasma wave propagation. When the reagent mixture enters the discharge region, the halogenides dissociate to form oxides, which are deposited on the inner surface of the tube. Thus, a 3- to 5-cm-long deposition zone arises at the head of the plasma column. To provide a 25- to 30-cm-long glass layer uniform in thickness, the deposition zone is periodically displaced back and forth along the tube by controllably varying the length of the plasma column. The plasma column length variation (plasma scanning) frequency was 20 Hz; the deposition zone displacement amplitude, 25 cm. (For a detailed description of the SPCVD setup, see [9]).

The composition of the glass deposited was specified by the ratio between the flow rates of halogenides ($SiCl_4$ and others). The reagent ratios were set by flow-rate controllers and controllers of the solid reagent temperature. The total flow rate of the gaseous reagents provided a rate of glass deposition of 2–3 μm/min. The thickness of the glass deposited was varied from 150 to 300 μm.

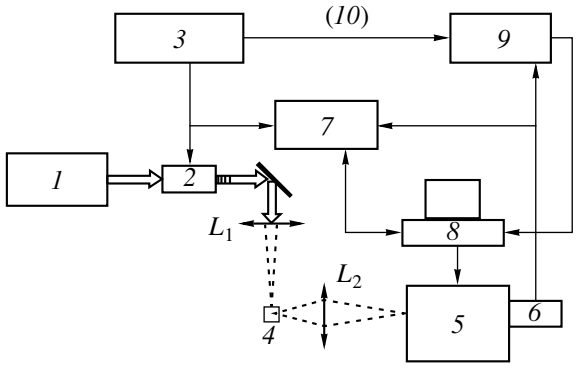

Fig. 1. Setup for studying the luminescent properties of the glasses.

An additional advantage of the SPCVD process over the other techniques of low-temperature synthesis of activated glasses is that it allows for obtaining glasses with a low concentration of Cl and an extremely low (≈1 ppm) concentration of OH hydroxyl groups, which adversely affect erbium luminescence [10].

The temperature of the substrate tube is a basic parameter governing the composition and properties of the glass. In the SPCVD process, the tube is heated by the plasma from within and by additional heating elements from without. During deposition, the mean time the inner surface of the tube is exposed to the plasma at the ends of the scan zone differs greatly, so that the temperature distribution along the substrate surface is highly nonuniform.

In our experiments, the desired temperature at the outer surface of the tube was kept accurate to ±1% with a feedback loop in the heater circuit. It was measured with an IRCON pyrometer at the site of the tube corresponding to the center of the scan zone.

The glass samples cut from the cross section of the tube had the form of 2-mm-thick semirings with polished end faces. They were selected from several experiments aimed at obtaining Er-doped glasses of different composition (see table). In a number of them, the temperature nonuniformity along the tube resulted in the corresponding composition nonuniformity with the ratio of the reagents entering the reactor kept unchanged. Because of this, the samples taken for spectroscopic studies were cut from different sections of the tube. The composition of the glass in each of the sections was examined with the X-ray microanalyzer of a JEOL JSM-5910LV electron microscope.

The luminescence from the samples was studied with the experimental setup shown in Fig. 1, which allows one to record luminescence spectra and measure the luminescence time. The radiation from cw Ar^+ laser *1* passes through a modulator consisting of electrooptic shutter *2* and driving generator *3* of rectangular pulses, is compressed by quartz lens L_1 and is applied to sample *4* vertically (parallel to the entrance slit of monochromator *5*). The modulator interrupts the pump radiation by rectangular pulses with leading-edge and trailing-edge times of 1 μs or shorter. Luminescence is excited over the deposited layer normally to the plane of the semiring. The diameter of the laser beam incident on the sample was no more than 150 μm, i.e., smaller than the thickness of the deposit. With regard to the focal length of lens L_1, ≈50 cm, the variation of the beam diameter over the sample can be neglected. Quartz lens L_2 transfers the image of the zone irradiated to the entrance slit of the monochromator. At the exit from the monochromator, the radiation is recorded by GaAs photodiode *6* (at wavelengths of 1000–1700 nm) or an FÉU-62 photomultiplier (in the wavelength range

Composition of the samples under study and the kinetic characteristics of photoluminescence due to the $^4I_{13/2}$–$^4I_{15/2}$ transition

Host	Er, ppm	F, wt %	N, at. %	K, mol %	Al, mol %	Ge, mol %	P, mol %	τ, ms
SiO_2, T_{depos} = 1200°C	1020							11.6
	990							11.5
	1280							11.5
F : SiO_2, T_{depos} = 1150°C	800	3.5						***
	640	3.2						***
	800	2						***
K : SiO_2, T_{depos} = 1050°C	2600			0.6				12
	1200			0.4				12.9
	1000			0.2				12.8
N : SiO_2, T_{depos} = 1230°C	240		3 +1.5 wt %Cl					
Al : SiO_2, T_{depos} = 1110–1230°C	1980				0.8			9.9
	1950				0.8			9.9
	2550				1.2			9.6
	3200				1.0			10.0
	3500				1.0			10.0*
	5400				1.2			9.5*
	7500				1.6			9.1*
P : SiO_2, T_{depos} = 1100°C	13000						6.5	5.8***
	13400						5.5	5.4***
	3600						6.5	8.9**
	3200						5.2	7.9**
	1800						4.6	8.7*
Ge : SiO_2, T_{depos} = 1220°C	1800					11		11.6*
	2300					15		11.6*
	3600					4		10.5**
	6450					4		11.3**
P, Al : SiO_2, T_{depos} = 1050°C	710				2.2		6	9.2
	2600				2.9		9.4	9.2*
	4100				2.6		10.5	8.9*
	5660				2.7		11.9	8.1*
	7100				2.7		12.8	7.74*
P, K : SiO_2, T_{depos} = 1020°C	2400			0.74			3.5	2.9
	3600			0.69			3.5	3.4*
	5360			0.52			5.3	6.3**
	7100			0.2			7.65	7.5**
	10760			0.1			10.1	7.11*
Ge, Al : SiO_2, T_{depos} = 1150°C	5600				2.6	16.1		8.9*
	5000				4	17.9		9
	2900				5.2	17.5		8.9

Note: */**/*** Slight/moderate/major contribution of the fast exponential to the kinetics of 1.53-μm luminescence.

800–1100 nm). The luminescence spectra are taken with EG&G5209 synchronous detector *7* controlled by computer *8*. The luminescence time is measured with SR250 gated integrator *9* synchronized (*10*) with the modulator. Near 1.53 μm, the measurements were made at a modulation frequency of 9 Hz; near 0.98 μm, at 110 Hz. The mean power of the pump beam at the output of the modulator was 250 mW.

SPCVD SYNTHESIS OF MULTICOMPONENT GLASSES

As has already been mentioned in the introduction, the SPCVD technology of glasses has a number of features, which show up most vividly in obtaining doped glasses [11]. It is known, for example, that the introduction of such elements as F, Ge, K, Al, and P into the silicate matrix to modify the glass reduces its viscosity. As the temperature of the substrate tube grows, compounds of these elements are desorbed from the surface at a higher rate, which decreases the doping level in the glass being deposited. A temperature gradient along the tube typical of the SPCVD process causes a corresponding longitudinal nonuniformity in the glass composition.

Since $ErCl_3$ evaporated at 1000°C in our experiments, we had to keep the temperature of the tube at a relatively high level throughout the deposition zone in order to prevent the condensation of the reagent. This may be a reason for an extremely low potassium concentration in the glasses deposited at this temperature (see table). Apparently, here we are facing the ability of alkali metals to significantly fluidize silicate glasses [12].

The temperature dependence of the incorporation efficiency of phosphorus in the temperature range 1000–1200°C is also very strong. Therefore, its concentration was controlled largely by the temperature of the tube during deposition.

A specific feature of nitrosilicate glass deposition is that the oxidation of silicon tetrachloride proceeds under the oxygen deficiency conditions [13]. Under such conditions, to reach a high level of codoping by other elements, such as Er, Ge, Al, etc., is a challenge because of the process chemistry. Furthermore, when oxygen is deficient in the glass, the concentration of harmful Cl rises drastically. As a result, the maximal erbium concentration in the nitrosilicate glass was as low as 240 ppm (1.6×10^{19} cm^{-3}).

The efficiency of incorporation of the elements into the silicate matrix depends not only on the temperature of the substrate tube and relative flow rate of the reagents but also on the composition of the glass being deposited. We relate this effect to the type of defect generated in the structural network of the glass by an element embedded in the glass. Note also that the incorporation efficiency correlates with the solubility of the corresponding oxide in SiO_2. For example, the efficiency of incorporation of erbium into the silicate and alumina–silicate matrices during SPCVD was ≈20% in our experiments. Due to a considerable structural disturbance, chemisorbed erbium and aluminum atoms turn out to be weakly bonded to oxygen on the silica glass surface. Weak bonding favors their desorption or substitution of silicon atoms for them. An increase in the aluminum halogenide flow rate versus that of $SiCl_4$ enhances light scattering in the glass, indicating the presence of the concentration homogeneity limit in SPCVD alumina–silicate glass. The addition of Ge generates network defects favorable to the incorporation of erbium and aluminum, as is confirmed by the rise in the incorporation efficiency for these elements to ≈50%. With phosphorus added to the silicate matrix, the incorporation efficiency of erbium rises still further (up to ≈100%). As follows from the table, codoping by phosphorus and aluminum doubles the maximal concentrations of both elements, presumably because a P–Al cluster is more readily incorporated into the silicate network. It should be noted that the obtaining of Al- and P-codoped SiO_2 glasses by means of the standard (nonplasma) MCVD technique is a big technological bugaboo.

Summing up, it may be said that the SPCVD technique as applied to multicomponent glasses is in a sense self-regulating; that is, the atomic packing is not too highly disturbed by thermal fluctuations and the structure of the glass is dense and perfect.

EXPERIMENTAL RESULTS

Figure 2 shows the luminescence spectra of erbium ions embedded in the fluorosilicate matrix. That taken at a low temperature is seen to consist of a number of closely spaced sharp lines. The long luminescence time at 0.98 μm indicates that, in this glass, unlike the rest of the glasses studied in this work, the multiphonon relaxation channel associated with the $^4I_{11/2}$ level is combated. The kinetics of luminescence near 1.53 μm features rapid relaxation mechanisms. The luminescence spectrum of Er^{3+} ions in the nitrosilicate matrix (Fig. 3) also comprises a series of sharp lines, which particularly stand out as the pump modulation frequency increases. In our opinion, these lines can be assigned to erbium ions with the shortest lifetime of the $^4I_{13/2}$ level. The spectrum at 0.98 μm has an extra peak at 1.001 μm. Unfortunately, we did not manage to determine the luminescence time in this case because of a low intensity of the signal.

Figures summarize the luminescence spectra taken from all the samples at 1.53 μm. They are normalized by their peak values for comparison convenience. Erbium ions in the F : SiO_2, Al : SiO_2, and Al, Ge : SiO_2 matrices have the broadest spectra (50, 47, and 47 nm wide, respectively). The spectrum taken from the K : SiO_2 matrix, conversely, is the narrowest (24 nm wide), and the luminescence time here is the longest. Such radical modifications of the luminescence pattern take place despite a low potassium concentration in the glass.

The luminescence spectra taken from the phosphorus-containing samples are similar to each other, but the luminescence kinetics in them is different. In the P, K : SiO_2 and P : SiO_2 glasses, the $^4I_{13/2}$ level lifetime decreases markedly with decreasing phosphorus concentration and increasing erbium concentration. At the

same time, the lifetime of this level in P, Al : SiO_2 depends only on the erbium concentration.

DISCUSSION

It was shown [14] that Er^{3+} ion clustering and its associated up-conversion are responsible for the slow component in the kinetics of luminescence at 0.98 μm. However, we did not observe this effect in the samples studied. The reasons may be the following: (i) the effect is too weak to be detected, (ii) the effect is distinct only in highly clustered glasses, and (iii) the fast processes observed in the kinetics of 1.53-μm luminescence are related to multiphonon transitions rather than to up-conversion.

Determining the absolute quantum efficiency of luminescence in thin layers is a bottleneck, since the absorbed pump power is difficult to measure. Since the luminescence excitation and recording conditions in our experiments were reproduced with an accuracy of 5%, we succeeded in making comparative estimates of the luminescence quantum efficiency. Figure 5 plots the relative quantum efficiencies of luminescence ($^4I_{13/2} \longrightarrow {}^4I_{15/2}$, λ = 1.53 μm) against the erbium concentration. The relative quantum efficiency was calculated by the formula

$$q_i = \frac{\mathrm{Lum}_i N_\mathrm{m}}{\mathrm{Lum}_\mathrm{m} N_i} = \frac{\sigma_i Q_i(H_{11/2}, {}^4I_{13/2})}{\sigma_\mathrm{m} Q_\mathrm{m}(H_{11/2}, {}^4I_{13/2})}, \qquad (1)$$

where $\sigma_{i,\,\mathrm{m}}$ are the composition-dependent cross sections of electron excitation by 514.5-nm radiation, $Q_{i,\,\mathrm{m}}$ are the probabilities that electrons excited to the level $H_{11/2}$ will transit to the level $^4I_{13/2}$ and then execute a radiative transition to the ground state, and N_i and N_m are the Er^{3+} ion concentrations in the ground state. Quantities Lum_m and N_m correspond to the sample exhibiting a maximal efficiency.

In the calculation, the total erbium concentration in the samples was used instead of the erbium ion concentration in the ground state (N_i, N_m). This restricts the validity of formula (1) to the case of weak optical excitation. As is known, the adverse effect of up-conversion on the luminescence quantum efficiency grows with excitation level. Of practical interest are the parameters of the glasses at an excitation level close to inversion. Therefore, the excitation level in our experiments was 50–60%, according to the pump power used. In this case, the error in the quantum efficiency calculated by formula (1) may reach 20% because of different rates of excitation relaxation to the ground level.

Let us see how the deposition conditions influence the luminescent properties of erbium in the glasses. The structure and composition of SPCVD silica glasses are governed by chloride heterogeneous oxidation, the mobility of chemisorbed atoms being dependent on

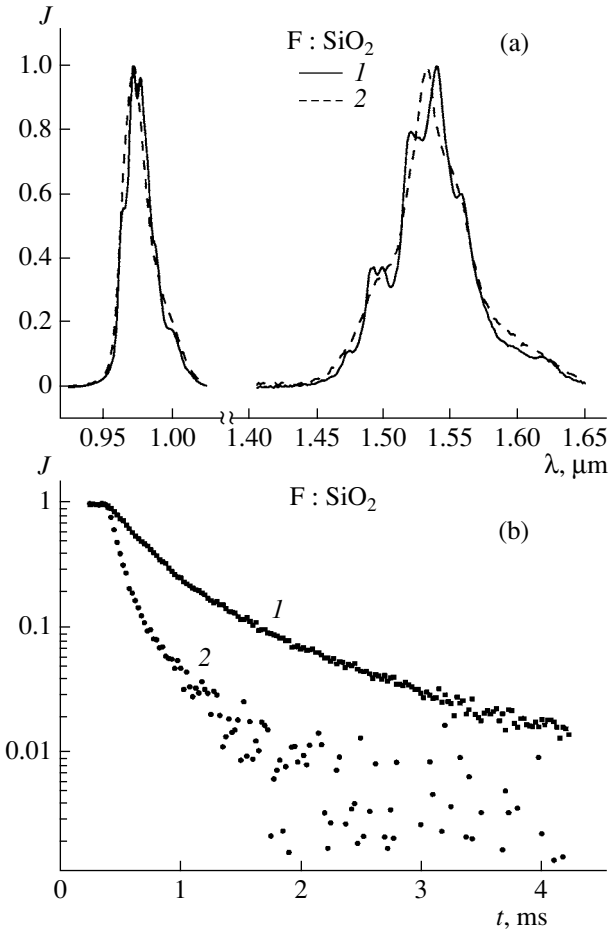

Fig. 2. (a) Spectra and (b) kinetics of Er^{3+} ion luminescence due to the $^4I_{11/2}$–$^4I_{15/2}$ transition (0.98 μm) for the fluorosilicate glass deposited at (*1*) low and (*2*) high temperature. The luminescence kinetics is approximated by a sum of two exponentials with indices (*1*) t_1 = 0.3 ms and t_2 = 1.23 ms and (*2*) t_1 = 0.09 ms and t_2 = 0.48 ms.

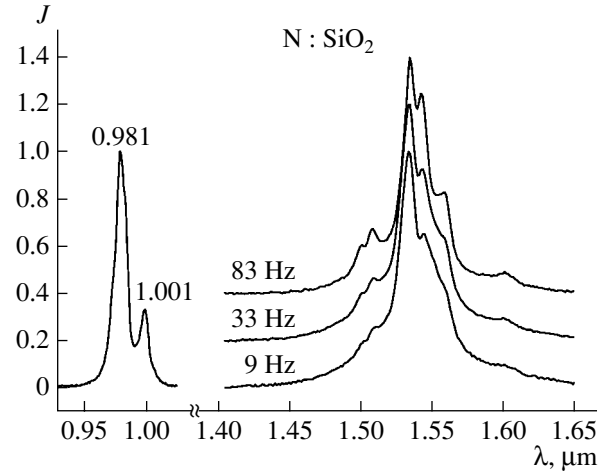

Fig. 3. Erbium luminescence spectra in the nitrosilicate glass at 0.98 and 1.53 μm for different pump modulation frequencies.

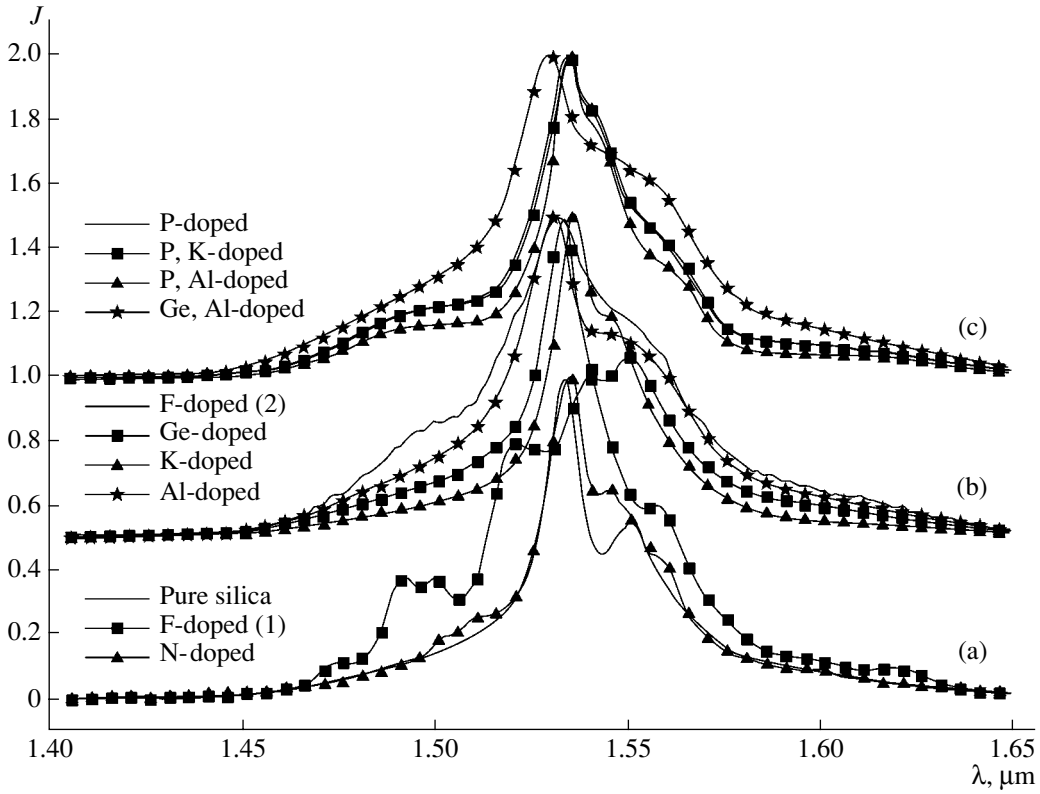

Fig. 4. Erbium ion luminescence spectra near 1.53 μm taken from the glasses of different composition.

substrate surface temperature T_{surf}. Three situations are worth considering here.

(1) $T_{surf} < T_{Er,Si}$ and T_X (X = Al, P, K, or Ge), where T_X is the characteristic temperature activating motion of the corresponding element in the glass. In this case, the atom mobility can be neglected and the structural network of the glass is governed by the particles from the gaseous phase that are "frozen" in the substrate surface. Under conditions (1), the glass is a thermodynamically nonequilibrium system. The complex luminescence spectra (Figs. 2, 3, and 5) reflect the contributions from different Er^{3+} ions in the structurally unstable anionic environment. For example, the complex shapes of the spectra shown in Fig. 2 indicate that the erbium ions are in the same anion environment, and the long lifetime of the state $^4I_{11/2}$, which is responsible for 0.98-μm luminescence, points to the presence of fluorine atoms in the environment [1]. The changes in the luminescence spectra taken from the nitrosilicate matrix seem to be due to chlorine and nitrogen atoms. Interestingly, when plotted as a function of the erbium concentration, the luminescence efficiency of all the glasses deposited under the conditions $T_{surf} < T_{Er,Si}$, T_X is fitted by a single straight line (Fig. 5). Thus, such conditions wipe out the difference between the glasses of different composition in this respect.

(2) $T_X < T_{surf} < T_{Er,Si}$. In this case, dopant atoms have a chance to occupy thermodynamically equilibrium and energetically favorable positions in the network of the glass. It is likely that setting the equilibrium structure is

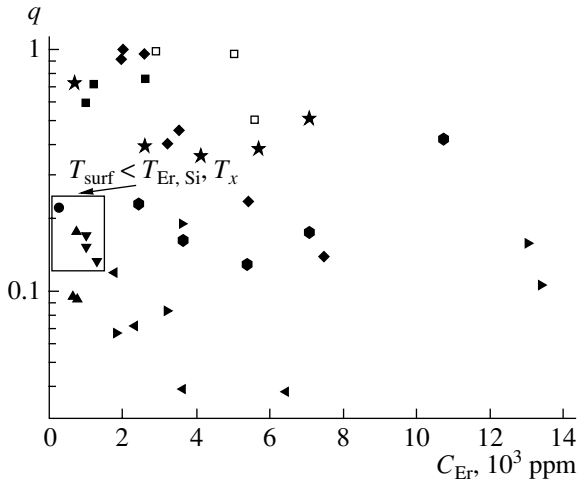

Fig. 5. Relative quantum efficiency of 1.53-μm luminescence (1000 ppm = 6.6×10^{19} cm^{-3}). (■) K-doped sample, (●) N-doped sample, (▲) F-doped sample, (▼) pure silica, (◆) Al-doped sample, (◀) Ge-doped sample, (▶) P-doped sample, (⬢) (P + K)-doped sample, (★) (P + Al)-doped sample, and (□) (Ge + Al)-doped sample.

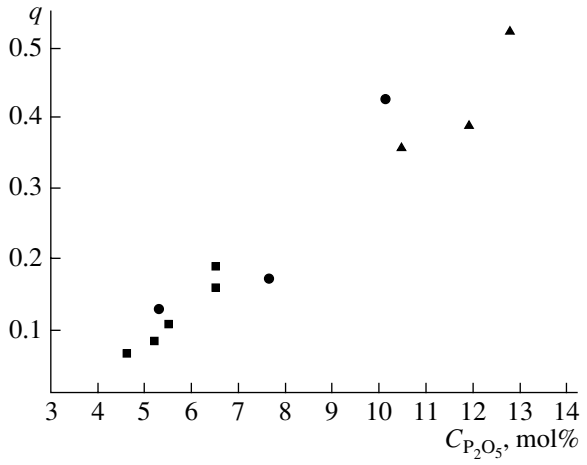

Fig. 6. Relative quantum efficiency of 1.53-μm luminescence vs. the phosphorus concentration. (■) P-doped, (●) (P + K)-doped, and (▲) (P + Al)-doped samples.

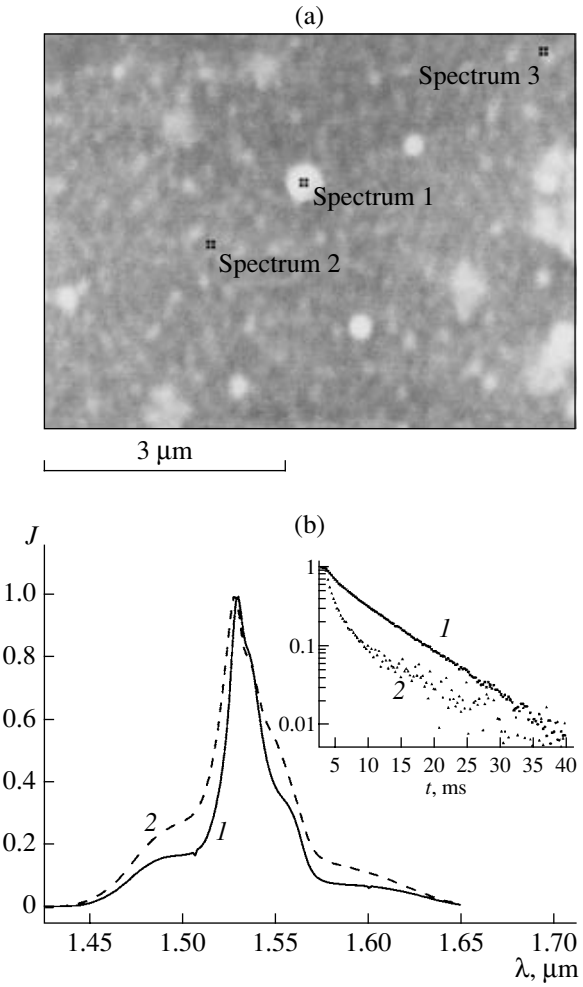

Fig. 7. Effect of fusion of the Al_2O_3(2.7 mol %)–P_2O_5(12.8 mol %)–Er(7100 ppm) glass on (a) clustering and (b) Er^{3+} luminescence parameters. The bright spots in panel (a) correspond to high-erbium areas. Panel (b) shows the luminescence spectra and kinetics for the sample obtained by plasma-chemical deposition (*1*) before and (*2*) after high-temperature treatment.

also accompanied by the motion of erbium atoms but only in the neighborhood of their initial positions. In this state, the structure of the specific glass volume (i.e., the volume containing a single erbium ion) is equilibrium and the glass as a whole may be viewed as thermodynamically quasi-equilibrium. Accordingly, the luminescence spectrum takes on the attributes of the typical luminescence spectrum of Er^{3+} ion in fused glasses. Almost all the glasses studied in this work were deposited under these temperature conditions. The spectrum (Fig. 3) and kinetics of 0.98-μm luminescence for the fluorosilicate matrix suggest that fluorine atoms leave the neighborhood of erbium at these temperatures.

(3) $T_{surf} > T_{Er}$ or T_{Si}. Under these conditions, erbium ions, when moving in the forming network of the glass, may generate clusters or even cause precipitation of Er_2O_3 in SiO_2 if their concentration is high.

The above concept of forming a homogeneous (cluster-free) structure of the glass may be invalid in some cases. Specifically, if the dopant concentration is high and $T_X \ll T_{surf}$ or the time of temperature action is long, the bulk of the glass may get mixed up well and thermodynamic equilibrium with clusters may set in the system even in the absence of activating motions of Er ions or Si atoms.

The luminescence pattern in the phosphosilicate glass is intriguing. Figure 6 plots the erbium luminescence quantum efficiency against the phosphorus concentration in the glass. From 5 mol % of phosphorus on, the quantum efficiency rises monotonically. Interestingly, while the high-phosphorus samples exhibit the best luminescence properties, those with a low phosphorus content are inferior to the other glasses in terms of the luminescent activity.

Figure 7 demonstrates changes in the spectrum and kinetics of erbium ion luminescence that arose when the samples were heated in the flame of an oxygen–propane burner. Softening of the glass is seen to cause erbium clustering. The luminescence spectrum broadens, and up-conversion signs appear in the kinetics pattern.

CONCLUSIONS

It was shown experimentally that moderate-temperature plasma-chemical deposition may serve as a basis for a new high-erbium glass synthesis technology. A high efficiency of luminescence due to the $^4I_{13/2}$–$^4I_{15/2}$ transition in these glasses offers considerable scope for designing active integrated optical systems. Of most interest are Al- and K-doped glasses obtained by the plasma-chemical technique. In these materials, the

quantum efficiency of luminescence remains high as the erbium concentration grows to at least 5000 ppm (3.3×10^{20} cm^{-3}). Halogens (F and Cl) introduced into the matrix adversely affect the quantum efficiency and reduce the concentration threshold of ion erbium clustering. It is demonstrated with the fluoro- and phosphosilicate composites that the luminescent properties of Er ions in unfused SPCVD glasses strongly depend on the substrate temperature during deposition. The optimal temperature is that at which the atomic structure in the neighborhood of an Er^{3+} ion becomes equilibrium but the activation motion of Er^{3+} ions in the matrix is still suppressed.

ACKNOWLEDGMENTS

This work was supported by the Russian Foundation for Basic Research, grant no. 04-02-16441.

REFERENCES

1. M. P. Hehlen, N. J. Cockroft, T. R. Gosnell, *et al.*, Opt. Lett. **22**, 772 (1997).
2. N. V. Nikonorov, A. K. Przhevuskii, M. Prassas, *et al.*, Appl. Opt. **38**, 6284 (1999).
3. M. P. Hehlen, N. J. Cockroft, T. R. Gosnell, *et al.*, Phys. Rev. B **56**, 9302 (1997).
4. A. K. Przhevuskii and N. V. Nikonorov, Opt. Mater. **21**, 729 (2003).
5. Y. B. Choi, S. H. Cho, and D. C. Moon, Opt. Lett. **25**, 263 (2000).
6. A. Polman, M. A. Marcus, and D. C. Jacobson, Mater. Res. Soc. Symp. Proc. **244**, 381 (1992).
7. D. Pavy, M. Moisan, F. Ould-Saada, *et al.*, in *Proceedings of the 12th European Conference on Optical Communication, Barselona, 1986*, pp. 19–22.
8. A. V. Kholodkov and K. M. Golant, in *Proceedings of the Optical Fiber Communications (OFC) Conference and Exhibition, Los Angeles, 2004*, Vol. 2, pp. 545–547.
9. E. M. Dianov, K. M. Golant, V. I. Karpov, *et al.*, Opt. Mater. **3**, 181 (1994).
10. Y. Yingchao, A. J. Faber, and H. de Waal, J. Non-Cryst. Solids **181**, 283 (1995).
11. A. V. Kholodkov, K. M. Golant, and I. V. Nikolin, Microelectron. Eng. **69**, 365 (2003).
12. M. E. Lines, J. Non-Cryst. Solids **171**, 209 (1994).
13. E. M. Dianov, K. M. Golant, R. R. Khrapko, *et al.*, J. Lightwave Technol. **13**, 1471 (1995).
14. A. V. Belov, in *Proceedings of the 11st International Conference on Integrated Optics and Optical Fiber Communication Combined with the 23rd European Conference on Optical Communication (IOOC-ECOC), 1997*, pp. 51–53.

Translated by V. Isaakyan